Nature Environment and Pollution Technology
An International Quarterly Scientific Journal

ISSN: 0972-6268	Vol. 15	No. 3	pp. 997-1004	2016

Original Research Paper

The Green Historic District Environment Protection and Utilization

Yangluxi Li
School of Architecture, Syracuse University, New York, USA

Nat. Env. & Poll. Tech.
Website: www.neptjournal.com

Received: 04-07-2015
Accepted: 07-10-2015

Key Words:
Green historic district
Natural ventilation
Wind environmen
Environment protection

ABSTRACT

The natural ventilation of a residential area has placed increasing emphasis on site planning, in order to find the relationship between natural ventilation and an effective site layout. This can reduce the energy consumption and the adverse effects of outdoor winds, improve the living environment and quality of life, as well as create harmony between humans and nature. In this paper, Air-Pak is used to simulate the wind environment of a residential area. Through analysing and simulating the airfield that forms when the wind blows around the residential buildings with Air-Pak, we explain the advantage of combining computer simulation software and residential area planning. Additionally, some advice is given regarding the layout of site design early in the planning phase using the simulation of buildings in the outdoor environment. An old historic city that needs reform, must aim to keep the history, address low-income resident living environments, and take into account the studio workshops. New buildings attract investment and development.

INTRODUCTION

In a time of economic instability and high unemployment, the public tendency is to search for new and old ideas to alleviate the uncertainty. How are we to build a sustainable economy from the current state of affairs? Many look towards new trends in localized industrial production combined with an increased interest in urban living and the customization from CNC or robotic manufacturing as indicators of the economy's condition (Bernard 2010). Should these prove as essential building blocks of a near future industry? How might the built environment anticipate this need?

Live·Make Industrial Arts Center, Cincinnati calls for architectural proposals for a membership based facility that will feature private residences, maker-in-residence studios, light industrial studios and an open workshop to help shape a new economic opportunity for the neighbourhood. The proposed site includes a building and undeveloped land. It is located in a neighbourhood of Cincinnati, Ohio recently designated as an 'Urban Mix' zoning area in order to encourage a return of manufacturing and living. This center will be a place for members to take advantage of evolving tools and modes of production from the past and present.

Proposals should recognize the history of innovation and civic engagement of the surrounding community as inspiration for the next generation to develop innovative ways of creative production that can impact the neighbourhood's future. The Industrial Arts Center, Cincinnati fits into the neighbourhood's master plan and could serve as a business and economic catalyst. It will be a community magnet and a center for production as other nearby sites are developed. The main objective is a contemporary architectural solution that engages the site's historic fabric and restores some of the original living and making characteristics of the community.

NEIGHBOURHOOD AND SITE

Over-the-Rhine: The geography of Cincinnati's basin has greatly impacted the location of housing and business development over the years. Fig.1 show the Over-the-Rhine's photograph by satellite and location. Before inclines, cable cars, and automobiles, it was far more difficult to navigate the hills surrounding the basin. This concentrated development and helped make Over-the-Rhine the most densely populated neighbourhood outside of lower Manhattan in the late 1800s. The historical significance of Over-the-Rhine was confirmed in 1983 when it was added to the National Register of Historic Places. At that time, the neighbourhood contained the largest collection of Italianate architecture in the country with more than nine hundred buildings.

Since the historical designation, many buildings have become abandoned and deteriorated because of neglect by individual building owners and non-profit entities that became overburdened or underfunded. A turning point came with protests, in 2001 and in 2006, when the United States National Trust for Historic Preservation listed Over-the-Rhine as one of the eleven most endangered historic places. Soon after, the efforts of private corporations and other organizations began reinvestment through major development

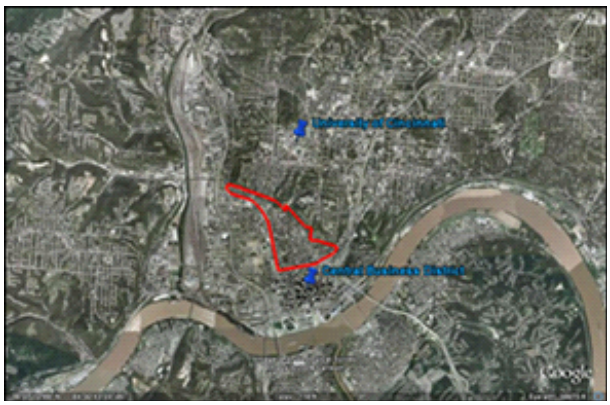

Fig.1: Over-the-Rhine's photograph by satellite and location.

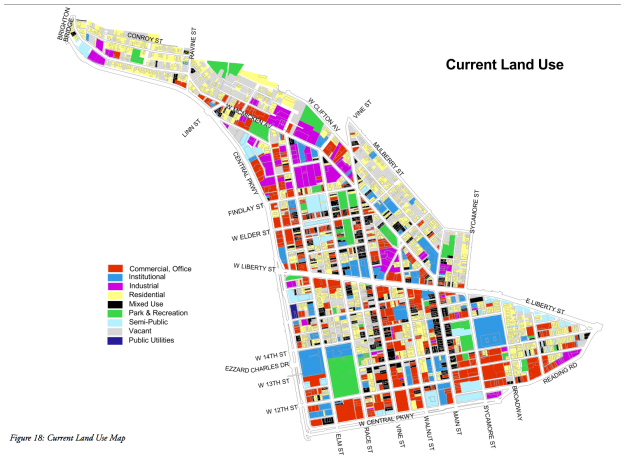

Fig. 2: Current land use map.

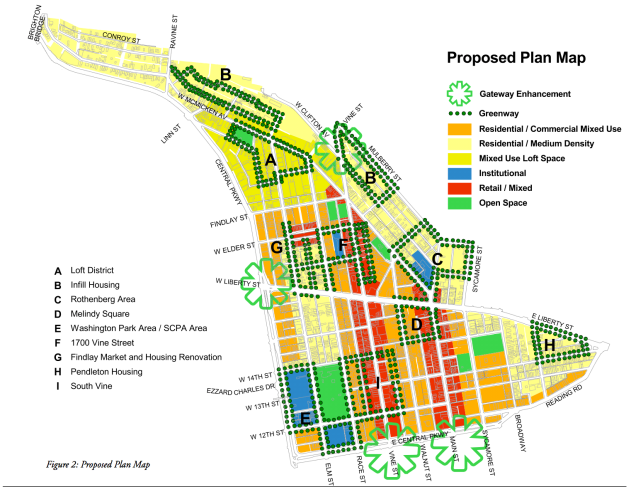

Fig. 3: Proposed plan map.

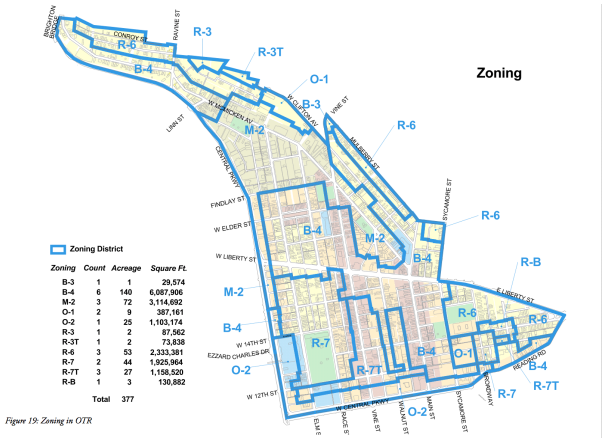

Fig. 4: Zoning in OTR.

and renovations, to help to change that designation.

Today Over-the-Rhine has become a community of restoration, renovation, and preservation, focusing on the importance of the neighbourhood as a whole over the individual building. Fig. 2 shows the current land use map, and Fig. 3 the proposed plan map.

Brewery district: Several distinct districts lie within Over-the-Rhine, including the Gateway Quarter, Pendleton District, Northern Liberties and the Brewery District. The proposed site for this competition sits within the Brewery District and will take advantage of the recent zoning change that the Brewery District Community Urban Redevelopment Corporation helped implement. The Urban Mix (UM) zone should provide a balance of vital economic, livable, and cultural opportunities to enhance the urban qualities. This new zoning designation should allow the Brewery District to function as it once was. Fig. 4 shows the Zoning in OTR.

126 W. McMicken: The competition site is located on the northern edge of the Brewery District at the base of a steep hill. This site will absorb the adjacent parcels to create a larger site, roughly 500ft by 150ft. The existing building on the site was originally built in 1900 as a 2-story structure for the Rapid Electrotype Company. It stands today as a damaged 1-story building due to a landslide in the 1970's. Fig. 5 shows the historical area bitmap, Fig. 6 the historical style facade and Fig.7 the historical view.

PROPOSAL

Program Overview

Live component: As a general theme, each housing unit should provide spaces for eating, sleeping, cooking, cleaning, gaming, relaxing, working, and gazing, rather than the traditional living room, dining room, bathroom and bedroom.

Fig. 5: Historical area bitmap.

Fig. 6: Historical style facade.

Fig.7: Historical view.

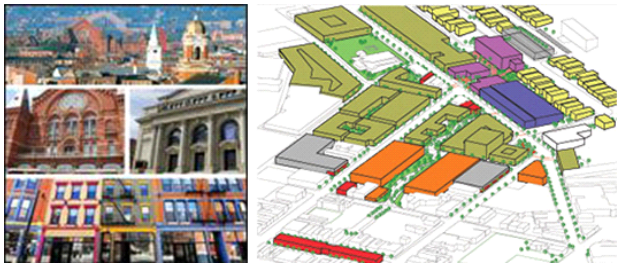

Fig. 8: Building space structure.

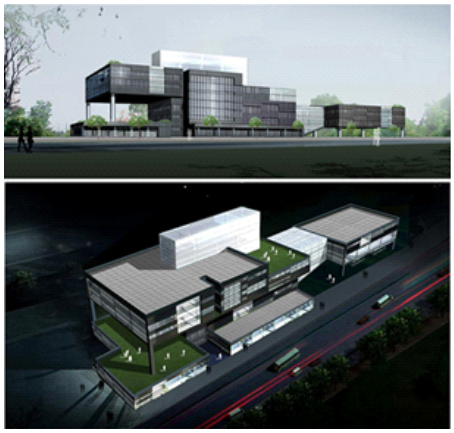

Fig. 9: New building effect diagram.

Fig. 10: Outdoor and indoor environment.

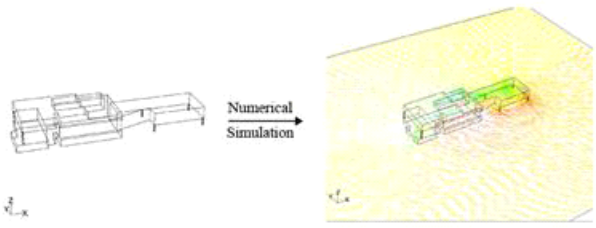

Fig. 11: Simulation by computer.

Fig. 8 shows the building space structure. It will be at the discretion of each individual entrant to define the level of details for each housing unit. At a minimum, the interior spaces should be generally designed and framed out for the anticipation of objects and design interventions. The housing units should engage the functions and goals of the MAKE component. The required number of housing units is set at a minimum of twelve and a maximum of thirty-six. Fig. 9 shows the new building effect diagram. In defining the number of housing units proposed, each entrant will have the opportunity to establish the importance and impact that the LIVE component will have on the overall program.

MAKE component: The Industrial Arts Center (IAC) Cincinnati, is a facility offering access to a variety of industrial machines and tools for artists, designers, engineers or anyone interested in the making of objects, goods, and products. The IAC will be a member-based workshop with hand-driven and computer-driven tools. The tools and machines available will vary greatly with both new and old technologies, but an emphasis on new methods of production is a key feature of this facility (I-Cheng 2006, Trcka et al. 2006).

In addition to the functions of the IAC, the building will house three key elements essential to the MAKE component

of the program. 1) Maker-in-Residence studios that would be granted to an individual for six months to one year. The IAC provides its resources to the Maker-in-Residence along with one housing unit on site. 2) Light Manufacturing Studios will create an everyday presence on site. These entities require dedicated tools or devices in house, but may also need access to the tools in the IAC. These studios can encourage start-up companies that are connected to or disconnected from the IAC, with their own private entry and exit. 3) Retail storefront will be a place for the community to interact with IAC member's productions and tools available for purchase. This public space is a place for items to be sold and ideas exchanged (Zhao et al. 2011). Fig 10 shows the outdoor and indoor environment.

THE ANALYSIS METHODS OF WIND ENVIRONMENT

The numerical simulation of the discrete fluid flow on the computer is used to solve for the airflow that follows the laws of fluid dynamics equations. Computer graphics technology also intuitively shows the results. This numerical simulation technology is known as the Computational Fluid Dynamics (CFD: Computational Fluid Dynamics) technology. This technology has a wide range of application in the manufacturing sector since 1974. However in recent years, researchers have applied CFD technology in simulation research work for the building environment. Currently, it has not been further applied or popularized, but it has made great development.

In this paper, Fluent software is used to do CFD analysis. This software uses many kinds of solving methods, as well as multiple grid accelerating convergence technology, to achieve the best convergence speed and precision. Fluent Air-pak is an artificial environment system analysis software for architects, engineers, designers, and other professional fields involving HVAC related work. It can accurately simulate effects of airflow, heat transfer and pollution physical phenomenon for research objects. This software can also simulate problematic airflow, air quality, heat transfer, pollution and comfort of ventilation systems, according to ISO 7730 standard supply comfort, PMV, and PPD technical indicators which measure the indoor air quality (IAQ) (Bert et al. 2011).

SIMULATION ANALYSIS

Model simply: The plane simulation result, with a distance of 1.6m from the ground, is selected for analysis. The main analysis will include the wind environment of the activities plane in the main building. Fig. 11 is an area CFD simulation simplified model. In the process of modeling, the main object of the analysis is the wind environment of the main building. The wind environment of the main building is the only one that needs to be considered without other buildings (Griffith 2002). As shown in Fig. 14, the model boundary size is: 127m×55m×4.5m; model scale is 1:1, the foundation is located at 0m.

Selection of numerical model: The turbulence model is one of the main components of the CFD software. The general CFD software is equipped with various levels of turbulence models that usually include the algebraic model, one and two equation models, the turbulent stress model and large eddy simulation. The wind flow of the construction area generally belongs to the incompressible flow with low and weak buoyancy turbulence. Commonly used mathematical models are standard K-μ model and large eddy simulation (LES). By contrast, the standard two equation model, or the K-μ model, has low computational cost, small fluctuations in the numerical calculation and high precision. It is also widely applied for low-speed turbulent number and is easy to use for network adaptations and complex community building shapes appropriate for unstructured grid (T grid) to mesh the surrounding fluid. Therefore, this paper uses the standard K-μ model. All of its governing differential equations include the continuity equation, momentum equation, K equation and μ equation. The formula is shown below considering the fluid incompressible, simplification after steady state:

(1) The turbulent viscosity coefficient.

$$\mu_t = \frac{C_\mu \rho k^2}{\varepsilon}$$

(2) The continuity equation

$$\frac{\partial(\rho u_i)}{\partial x_i} = 0$$

(3) The momentum equation

$$\frac{\partial(\rho u_i u_j)}{\partial x_i} = \frac{\partial}{\partial x_i}(\mu \frac{\partial u_i}{\partial x_j}) - \frac{\partial P}{\partial x_j}$$

(4) The K equation

$$\frac{\partial(\rho k u_i)}{\partial x_i} = \frac{\partial}{\partial x_i}[(\mu + \frac{\mu_t}{\sigma_k})\frac{\partial k}{\partial x_j}] + \mu_t(\frac{\partial u_i}{\partial x_j} + \frac{\partial u_j}{\partial x_i})\frac{\partial u_i}{\partial x_j} - \rho\varepsilon$$

(5) The μ equation

$$\frac{\partial(\rho \varepsilon u_i)}{\partial x_i} = \frac{\partial}{\partial x_j}[(\mu + \frac{\mu_t}{\sigma_\varepsilon})\frac{\partial \varepsilon}{\partial x_j}] + \frac{C_{1\varepsilon}\varepsilon\mu_t}{k}(\frac{\partial u_i}{\partial x_j} + \frac{\partial u_j}{\partial x_i})\frac{\partial u_j}{\partial x_i} - C_{2\varepsilon}\rho\frac{\varepsilon^2}{k}$$

The meaning of each item in the equation (4) and (5): from left to right are, the convection item, diffusion item, produce item, and dissipative item. In the formula, *u* is the fluid dynamic viscosity (the subscript t means turbulent

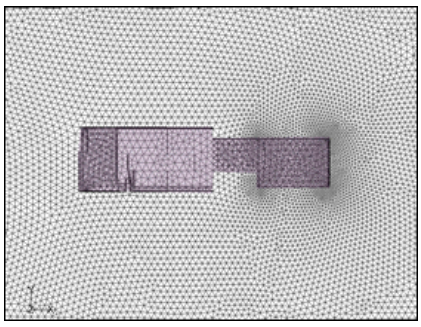

Fig. 12: Non-configuration mesh.

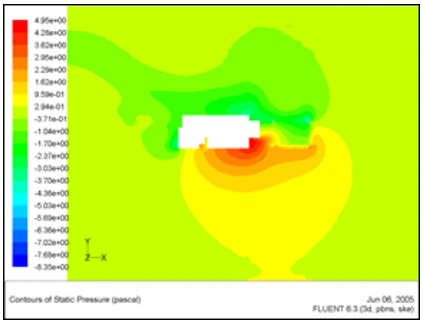

Fig. 13: 1.6 meters high wind pressure plan.

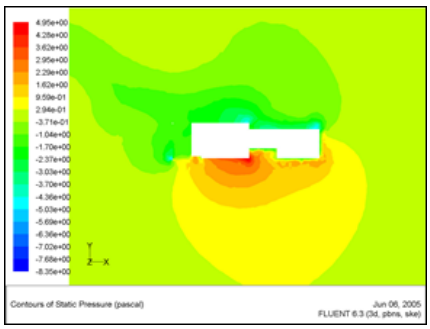

Fig. 14: 10 meters high wind pressure plan.

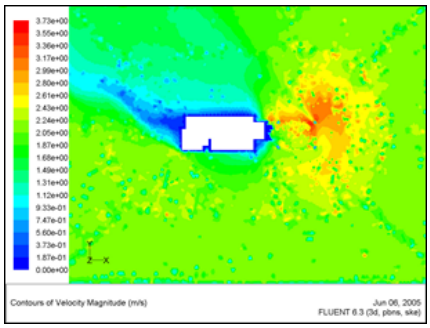

Fig. 15: 1.6 meters high wind velocity plan.

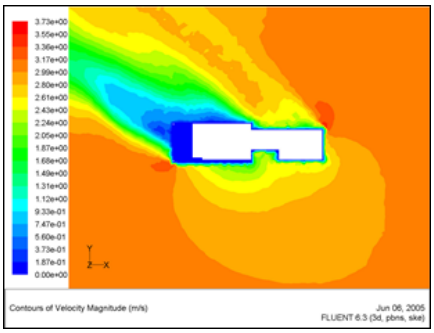

Fig. 16: 10 meters high wind velocity plan.

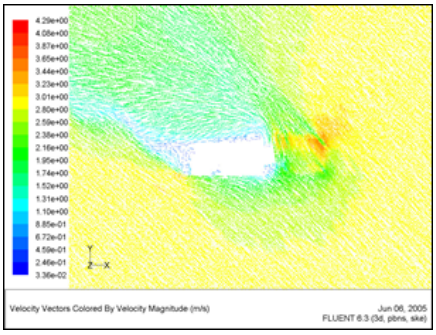

Fig. 17: 1.6 meters high wind vector diagram.

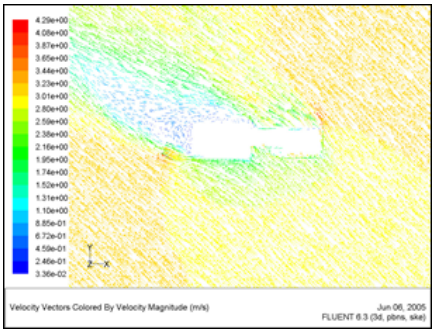

Fig. 18: 10 meters high wind vector diagram.

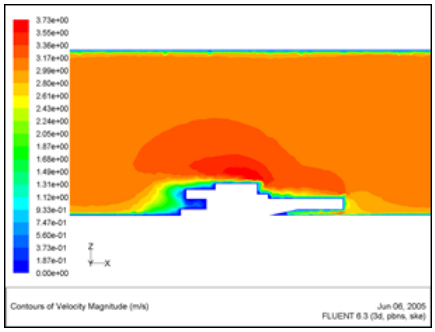

Fig. 19: Cross section wind vector plan.

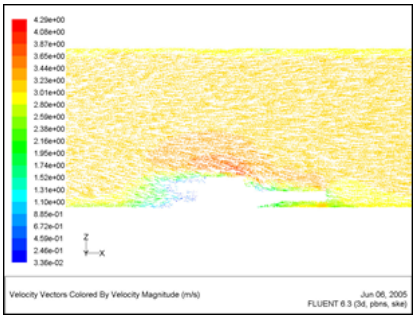

Fig. 20: Cross section wind vector diagram.

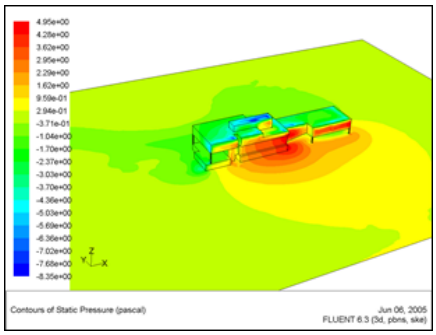

Fig. 21: 3D wind pressure plan.

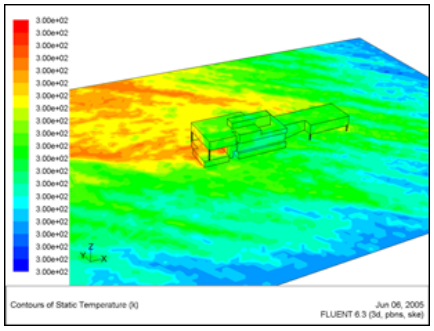

Fig. 22: 3D temperature plan.

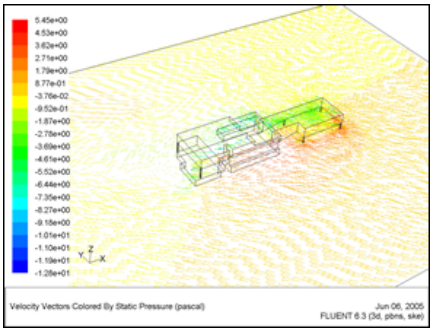

Fig. 23: 3D wind vector diagram.

flow); p is fluid density, unit is m^3/s; c_u is empirical constant; k is turbulent pulsating kinetic energy; ε is dissipation rating; u_i is temporal average velocity; σ_k and σ_μ correspond to the Prandtl number of turbulent pulsating kinetic energy k and dissipation rating ε; i and j are tensor indicators, data range (1, 2, 3). According to relevant provisions of the tensor, when the indicator of expressions is repeated twice, this equation is to be put within the scope of the index value of add and traversal. According to the recommended value of Launder and the later experiment, the model constant $C_{1\varepsilon}$, $C_{2\varepsilon}$, c_u, σ_k, σ_μ's values respectively are: $C_{1\varepsilon}$= 1.44; $C_{2\varepsilon}$= 1.92; c_u= 0.09; σ_k= 1.0; c_u=1.3 (Blocken et al. 2009, Yang & Wang 2013).

Boundary conditions and meshing: After the mathematical model and control equations are determined, the reasonable boundary conditions are determined to make the simulation experiment similar to real conditions. Analysis of the wind velocity and direction is done using the research institution's location. The wind velocity and direction frequency diagram is used, as mentioned above, to determine wind direction and velocity for the input conditions of the simulated region. In the calculation, the defined inlet is the velocity boundary condition of Fluent (velocity-inlet), calculated for summer typical working conditions (southeaster wind, wind velocity 3m/s) and typical winter working conditions (northwester winter, wind velocity 3m/s). In the calculation of this paper, the free flow boundary condition is defined as the outlet assuming the flow of the stream surface has been fully developed, and the normal flow is restored without the building block. The outlet relative pressure should be zero (Hooff et al. 2011, Tominaga et al. 2008). The building and ground surface is fixed, therefore the no slip wall condition is used. The wall is a kind of boundary condition to limit fluid and solid regions. For the viscous fluid adhesion condition, namely, consider the fluid velocity of mural face is the same as the velocity of the place of the mural face (front facade), no slip wall's velocity is zero, and the fluid velocity of mural face is zero.

Fluent software has mesh generation (pre-processing) and flow visualization (post-processing) modules, and the grid is divided into two categories: structural and non structural. The quality of grid generation has a significant effect on calculation precision and stability. Grid generation is also an important factor to measure CFD general software performance (Gromke et al. 2008, Fang et al. 2006, Johansson 2001). When using Air-pak for simulation in this research, the unstructured grid technique is used for the mesh grid. The meshed grid includes a variety of shapes, thus can maximize the visualization of the complex underlying surface shape and improve the effect of the model simulation (Fig. 12). The unstructured grid (T grid) is not restricted by the topology of the solution domain and boundary shape. Building it is very convenient, beneficial for generating the adaptive grid, and it can function according to the flow field characteristics of automatically adjusted grid density. It is very beneficial for improving accuracy of the local area calculation (Galbraith et al. 1997, EL Diasty 1996).

Simulation result and analysis: Fig. 13 and Fig. 14 show the wind pressure plans of the research institute at the height of 1.5m and 10m. Seen from the figure, in the summer, the southeast of the research institute is the windward side. At 1.5m, the wind field's static pressure and total pressure was between 1pa to 5pa. The maximum wind pressure appeared in the depression of the building on the windward side. Here, the wind pressure reached 5pa. The wind pressure of the first floor empty area and the building's leeward side was very small, around 0pa. This pressure difference is beneficial to the building's natural ventilation and pollutant dispersal. Seen from Fig. 14, the wind pressure of the research institute at 10m high was smaller than 1.5m. It was between 0.3pa to 4.5pa. This is caused by differences in the building's structure and facade.

Fig. 15 and Fig. 16 show the wind velocity plans of the research institute at 1.5m and 10m heights. The northwest side of the research institute has a long strip wind shadow with a wind velocity between 0-1.5m/s. The maximum wind velocity appeared in the northeast of the building, where the wind velocity reached 3.6m/s. With the building's height increased, the surrounding wind velocity gradually strengthened at the 10m high point of the research institute building (Fig. 16). Downstream of the building two wind velocity strengthened areas also appeared; the wind shadow area of the buildings backside (affected by building, there formed a wind velocity serious decline area at its backside) range is significantly larger, wind shadow area shape from the narrow slightly wider, in the middle part, wind velocity growth is not obvious, the wind velocity of two sides obviously increasing (Lee 2000, Francisco 2004). Fig. 17 and Fig. 18 show the wind direction vector at 1.5m and 15m heights at the research institute. Seen from the figures, wind across 1.5m exists in an empty place, where wind velocity increased along the mural face to the wind shadow area and several vortexes were formed. At the height of 10m, wind across through both sides of the building, formed shunt, wind shadow area formed a regular backflow vortex (Cheng 2013, Mistriotis et al . 1997, Boulard et al. 1999).

Fig. 19 and Fig. 20 show research of the cross section in the wind velocity plan and wind direction vector diagram. Airflow on the windward face stagnant area appeared shunt, did not produce the vortex, and was separated in front of the

top flange angle. There is an obvious strong vortex on the leeward side, which has a height taller than the top of the building. The wind velocity maximum that appeared at the top flange angle is 3.75m/s (Lucas 2004). Along the direction of the building height, wind velocity with the height appeared as the exponential law of growth rule. Therefore, the wind velocity at the bottom and depression were quite small; between 0-0.56m/s. Thus, this made the positive wind pressure coefficient smaller at the top of the building, although the wind velocity was higher. This is due to the 3D effect of the fluid airflow around the roof, and the decrease of the positive wind pressure coefficient. Therefore, the positive wind pressure coefficient presents the changing trend of big, middle, and small on both ends.

Fig. 21 to Fig. 23 show the stereoscopic wind pressure, wind direction and temperature of the Yuexi administrative district. Through elevation and stereoscopic image analysis, a more intuitive understanding can be achieved of the wind environment distribution around the research institute and the wind environment condition of the building area. We are also able to verify the space-changing rule of the airflow field, thus we can see: (1) The wind velocity maximum appears at the top front edge angle. (2) The wind pressure at the depression of the building is the maximum, but the wind pressure in the empty area is very small while the temperature is very high.

CONCLUSION

This paper uses a research institute for the example simulation. Numerical simulation method is completed in order to analyse the surrounding wind environment of the research institute. The numerical simulation can comprehensively gain the wind velocity and flow condition surrounding the building, and provide the basis for wind environment assessment. This simulation is a feasible and effective method. Using a reasonable boundary condition and turbulence model we were able to gain the reasonable fluid field distribution. For example, in the summer when the windward side wind velocity is 3m/s, the building's surrounding wind environment's velocity and pressure field can be found. Through analysis, the building's irregular areas, including the building's geometric profile, have a very large effect on its surrounding wind field, asymmetric geometry structure, and corresponding symmetrical geometry structure's surrounding wind fields are quite different. (1) On the leeward side of the building, affected by building's shape, an area of wind velocity with serious decline is formed. The range is greater, and the wind shadow area shape changes with the building's height and shape. (2) The building's windward side static pressure and backside negative existing pressure difference is significant. This is beneficial to natural ventilation; the wind velocities on the building's sides are higher, but at 1.5m (pedestrian height) they are smaller than 5m/s, and meet the requirement of comfort standard research. The negative pressure and strong vortex that exists on the backside does not benefit pollution discharge. Therefore, during building planning layout, the pollution accumulation here should be addressed.

ACKNOWLEDGEMENTS

This work was financially supported by the patents of ZL 201320138568.0 and ZL 201320138582.0.

REFERENCES

Bert, B., Ted, S., Jan, C. and Jan, H. 2011. Application of CFD in building performance simulation for the outdoor environment: an overview. Journal of Building Performance Simulation, 4(2): 157-184.

Blocken, B. and Persoon, J. 2009. Pedestrian wind comfort around a large football stadium in an urban environment: cfd simulation, validation and application of the new dutch wind nuisance standard. Journal of Wind Engineering and Industrial Aerodynamics, 97: 255-270.

Boulard, T., Haxaire, R. and Lamrani, M. A. et a1.1999. Characterization and modeling of the fluxes induced by natural ventilation in a greenhouse. Journal of Agricultural Engineering Research, 74: 135-144.

Cheng, H. 2013. Evaluating the performance of natural ventilation in buildings through simulation and on-site monitoring. Massachusetts Institute of Technology.

EL Diasty R., P. Fazio and I. Budaiwi.1996. The dynamic modeling of air humidity behaviour in a multi-zone space. Building and Environment, 28(1): 33-51.

Fang, Y., Campbell, M. and Ma, B. 2006. Probability map building algorithms design for an unknown dynamic environment. Intelligent Robots and Systems, 2006 IEEE/RSJ International Conference on (pp. 4736-4741).

Francisco, D.M., Diege, L.V. and Antonio, J.A. 2004. Measurement and simulation of climate inside Almeria-type greenhouses using computational fluid dynamics. Agricultural and Forest Meteorology, 125: 33-51.

Galbraith, G. H., McLean, R. C., and Guo, J. 1997. The selection of appropriate flow potentials for moisture transport models. IBPSA 5eme International Conference, Volume II, Prague, pp. 8-10.

Griffith, B. T. and Chen, Q. 2002. Incorporating nodal and zonal room air models into building energy calculation procedures. Massachusetts Institute of Technology.

Gromke, C., Buccolieri, R., Di Sabatino, S. and Ruck, B. 2008. Dispersion study in a street canyon with tree planting by means of wind tunnel and numerical investigations-evaluation of CFD data with experimental data. Atmospheric Environment, 42(37): 8640-8650.

Hooff, T. V., Blocken, B., Aanen, L. and Bronsema, B. 2011. A venturi-shaped roof for wind-induced natural ventilation of buildings: wind tunnel and cfd evaluation of different design configurations. Building and Environment, 46(9): 1797-1807.

I-Cheng, Y. 2006. Architectural layout optimization using annealed neural network. Automation in Construction, 15(4): 531-539.

Johansson, L. and Westerlund, L. 2011. Energy saving in indoor swimming-pools: comparision between different heat-recovery systems. Applied Energy, 70: 281-303.

Lee, I.B., Short, T.H. 2000. Two-dimensional numerical simulation of natural ventilation in a multi-span greenhouse. Transaction of ASAE, 43(3): 745-753.

Li, Yangluxi 2012. Analysis of planning of neighborhood communication space in the livable community. Applied Mechanics and Materials, 174-177.

Lucas, F. and Miranville, F. 2004. Indoor humidity modeling and evaluation of condensation on interior surfaces. Ashrae Transactions, 110: 300-308.

Mistriotis, A., Bot, G.P.A., Picuno, P. and Scarascia-Mugnozza, G. 1997. An alysis of the efficiency of greenhouse ventilation using computational fluid dynamics. Agricultural and Forest Meteorology, 85: 217-228.

Tominaga, Y., Mochida, A., Yoshie, R., Kataoka, H., Nozu, T., Yoshikawa, M. and Shirasawa, T. 2008. AIJ guidelines for practical applications of cfd to pedestrian wind environment around buildings. Journal of Wind Engineering & Industrial Aerodynamics, 96: 1749-1761.

Trcka, M., Hensen, J.L.M. and Wijsman, A.T.M. 2006. Distributed building performance simulation - a novel approach to overcome legacy code limitations. HHVAC&R Research, 12(S1): 621-640.

Yang, R. and Wang, L. 2013. Multi-zone building energy management using intelligent control and optimization. Sustainable Cities & Society, 16-21.

Zhao-Lin, Gu, Yun-Wei, Zhang, Yan, Cheng and Shun-Cheng, Lee 2011. Effect of uneven building layout on air flow and pollutant dispersion in non-uniform street Canyons. Building and Environment, 29(3): 2657-2665.